Transcriptional regulation of Munc13-4 expression in cytotoxic lymphocytes is disrupted by an intronic mutation associated with a primary immunodeficiency

Frank Cichocki,[1,3] Heinrich Schlums,[1] Hongchuan Li,[4] Vanessa Stache,[1] Timothy Holmes,[1] Todd R. Lenvik,[3] Samuel C.C. Chiang,[1] Jeffrey S. Miller,[3] Marie Meeths,[2,5] Stephen K. Anderson,[4] and Yenan T. Bryceson[1,6]

[1]Centre for Infectious Medicine, Department of Medicine; [2]Clinical Genetics Unit, Department of Molecular Medicine and Surgery, and Center for Molecular Medicine, Karolinska Institutet, Karolinska University Hospital Huddinge, 141 86 Stockholm, Sweden
[3]Division of Hematology, Oncology and Transplantation, University of Minnesota Cancer Center, Minneapolis, MN 55455
[4]Basic Science Program, Leidos Biomedical Research, Inc., Laboratory of Experimental Immunology, SAIC-Frederick Inc., Frederick National Laboratory, Frederick, MD 21702
[5]Childhood Cancer Research Unit, Department of Women's and Children's Health, Karolinska Institutet, Karolinska University Hospital Solna, 171 76 Stockholm, Sweden
[6]Broegelmann Research Laboratory, Clinical Institute, University of Bergen, N-5021 Bergen, Norway

Autosomal recessive mutations in *UNC13D*, the gene that encodes Munc13-4, are associated with familial hemophagocytic lymphohistiocytosis type 3 (FHL3). Munc13-4 expression is obligatory for exocytosis of lytic granules, facilitating cytotoxicity by T cells and natural killer (NK) cells. The mechanisms regulating Munc13-4 expression are unknown. Here, we report that Munc13-4 is highly expressed in differentiated human NK cells and effector CD8$^+$ T lymphocytes. A *UNC13D* c.118-308C>T mutation, causative of FHL3, disrupted binding of the ETS family member ELF1 to a conserved intronic sequence. This mutation impairs *UNC13D* intron 1 recruitment of STAT4 and the chromatin remodeling complex component BRG1, diminishing active histone modifications at the locus. The intronic sequence acted as an overall enhancer of Munc13-4 expression in cytotoxic lymphocytes in addition to representing an alternative promoter encoding a novel Munc13-4 isoform. Mechanistically, T cell receptor engagement facilitated STAT4-dependent Munc13-4 expression in naive CD8$^+$ T lymphocytes. Collectively, our data demonstrates how chromatin remodeling within an evolutionarily conserved regulatory element in intron 1 of *UNC13D* regulates the induction of Munc13-4 expression in cytotoxic lymphocytes and suggests that an alternative Munc13-4 isoform is required for lymphocyte cytotoxicity. Thus, mutations associated with primary immunodeficiencies may cause disease by disrupting transcription factor binding.

CORRESPONDENCE
Yenan T. Bryceson:
yenan.bryceson@ki.se

Abbreviations used: ChIP, chromatin immunoprecipitation; ENCODE, Encyclopedia of DNA Elements; FHL, familial hemophagocytic lymphohistiocytosis; PID, primary immunodeficiency; SNF, Switch (swi)-sucrose nonfermenter.

Dissection of the genetic susceptibility of humans to infections has provided fundamental insights into immunology, in addition to facilitating the diagnosis and treatment of several primary immunodeficiency diseases (PIDs; Casanova and Abel, 2004). Studies of familial hemophagocytic lymphohistiocytosis (FHL), an early onset, often fatal, hyperinflammatory and lymphoproliferative syndrome frequently triggered by viral infections, have delineated several genes required for lymphocyte cytotoxicity (Janka, 2012). FHL is now known to be associated with autosomal recessive mutations in *PRF1*, *UNC13D*, *STX11*, and *STXBP2* (de Saint Basile et al., 2010). Notably, patients with hypomorphic mutations in these genes may also present with malignancies later in life (Brennan et al., 2010).

H. Schlums and H. Li contributed equally to this paper.

Supplemental material can be found at:
http://doi.org/10.1084/jem.20131131

The Rockefeller University Press $30.00
J. Exp. Med. 2014 Vol. 211 No. 6 1079-1091
www.jem.org/cgi/doi/10.1084/jem.20131131

Despite the abundance of tests that are available to diagnose genetic diseases, definitive mutations are not found for 30–50% of patients that present with a single-gene disorder. This fact may be due to the failure to detect mutations in functional elements that lie outside of the coding region for a given gene when screening for mutations using whole-exome sequencing (Fratkin et al., 2012; Yang et al., 2013). The Encyclopedia of DNA Elements (ENCODE) project suggests that a considerable percentage of the human genome outside of coding regions consists of functional elements that are involved in regulating gene expression in a tissue-specific manner across cell types (Thurman et al., 2012). These functional elements are generally found in areas that are enriched for open chromatin, histone modifications, and transcription factor binding sites. Thus, to provide an accurate diagnosis in a greater number of PID patients, a deeper understanding of cis-regulatory elements and their role in gene regulation is necessary.

UNC13D mutations, associated with FHL type 3 (FHL3, MIM 608898), have been estimated to account for up to 32% of the reported cases of FHL, and a variety of nonsense and missense *UNC13D* mutations have been identified (Feldmann et al., 2003; Santoro et al., 2008). In humans, *UNC13D* comprises a coding sequence of 3,273-bp distributed over 32 exons and spanning 14 kb on chromosome 19 (Koch et al., 2000). It encodes Munc13-4, a protein required for cytotoxic T cell and NK cell degranulation, but also critical for degranulation by other hematopoietic cell types. In Munc13-4–deficient cytotoxic lymphocytes, secretory lysosomes can dock onto, but do not fuse with, the plasma membrane (Feldmann et al., 2003). Munc13-4 has dual functions as it also promotes the attachment of recycling and late endosome structures, which makes a pool of vesicles available to be used in the regulated exocytic pathway (Ménager et al., 2007; Wood et al., 2009).

We recently identified a single nucleotide mutation in intron 1 of *UNC13D* in FHL3 patients that, without affecting splicing, leads to a significant decrease in the levels of *UNC13D* transcripts in lymphocytes. The intron 1 mutation is causative of disease in many Caucasian patients across Europe and North America (Meeths et al., 2011). An identical but independently arising mutation was recently described as disease causing in Korean FHL3 patients (Seo et al., 2013), and an adjacent mutation was identified in an FHL3 patient from Singapore (Entesarian et al., 2013). These findings led us to hypothesize that a regulatory element critical for Munc13-4 expression could be located in intron 1 of *UNC13D*.

Here, we show that an intronic *UNC13D* regulatory sequence, bound by transcription factors ELF1 and STAT4, represents an enhancer promoting an open chromatin environment permissive for active gene transcription and Munc13-4 expression, as well as a novel alternative promoter driving expression of a distinct Munc13-4 isoform. These insights into regulation of Munc13-4 expression provide a deeper understanding of how defects in gene regulation can cause PID. Furthermore, our results reveal a novel role for STAT4 in programming of human naive T lymphocytes for cytotoxicity downstream of TCR engagement.

RESULTS

Munc13-4 expression levels correlate with cytotoxic lymphocyte differentiation

Understanding how Munc13-4 expression is controlled in distinct lymphocyte subsets is of interest considering the pivotal role of this protein for lymphocyte cytotoxicity (Feldmann et al., 2003). A ubiquitous Munc13-4 expression pattern was initially reported by Koch and colleagues (Koch et al., 2000), but a more detailed analysis has not since been performed. To compare Munc13-4 expression levels between cytotoxic and noncytotoxic lymphocytes, we isolated lymphocyte subsets from the peripheral blood of healthy donors and performed Western blots for Munc13-4. Relative to $CD19^+$ B cells, $CD3^-CD56^+$ NK cells expressed very high levels of Munc13-4. Moreover, $CD4^+$ T cells expressed low levels of Munc13-4, whereas total $CD8^+$ T cells expressed intermediate levels. To determine whether Munc13-4 is concomitantly induced along with the acquisition of lytic granules, we compared expression in $CD56^{bright}$ and $CD56^{dim}$ NK cells as well as in naive and effector $CD8^+$ T cells. In both NK cells and $CD8^+$ T cells, maturation and acquisition of lytic granules was associated with a marked increase in Munc13-4 expression, indicating that Munc13-4 is up-regulated during differentiation of cytotoxic lymphocyte subsets (Fig. 1, a and b). High levels of Munc13-4 expression thus correlate with a strong propensity to degranulate in response to engagement of activating receptors on cytotoxic T cells or NK cells (Chiang, et al., 2013). Notably, expression levels of syntaxin-11 and Munc18-2, also encoded by genes associated with FHL, were less correlated with cytotoxicity in lymphocyte subsets (Fig. 1, a and b). Thus, the data suggest an important role for induction of Munc13-4 expression in regulating the cytotoxic capacity of lymphocytes.

A c.118-308C>T mutation in intron 1 of *UNC13D* disrupts ELF1 binding to an evolutionarily conserved enhancer and lymphocyte-specific alternative promoter

The marked increase in Munc13-4 expression upon differentiation indicated that lineage-specific mechanisms promote high levels of Munc13-4 expression. Recently, we identified a c.118-308C>T mutation in an evolutionarily conserved region deep within intron 1 of *UNC13D* (Fig. 2 a) in patients with FHL3 that leads to a lymphocyte-specific loss of Munc13-4 expression (Meeths et al., 2011). NK cells from these individuals exhibit defective degranulation (Fig. 2 b). These results led us to hypothesize that a regulatory region critical for Munc13-4 expression in cytotoxic lymphocytes is located within intron 1 of *UNC13D*. We used transcription factor binding prediction software (Heinemeyer et al., 1998) to identify potential binding sites within intron 1 of *UNC13D* that might be disrupted by the mutation and found that a consensus ETS site overlaps with the location of the c.118-308C>T mutation (Fig. 2 c). To determine whether an ETS family member binds to this site, we synthesized wild-type and mutant oligonucleotide probes corresponding to the sequences shown in Fig. 2 a for use in EMSAs with nuclear lysates from primary NK cells and the NK92 cell line. A clearly discernable

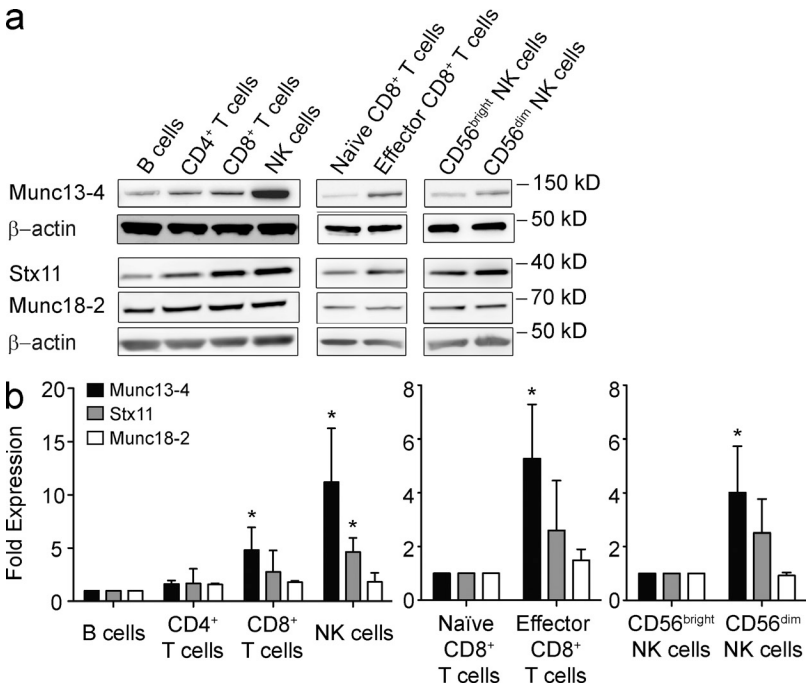

Figure 1. Munc13-4 expression levels correlate with lymphocyte cytotoxicity. (a) Western blot analysis of Munc13-4, Stx11, and Munc18-2 expression in eight different isolated subsets of human peripheral blood lymphocytes from a healthy peripheral blood donor. All cell types were isolated by negative magnetic bead selection except for $CD56^{bright}$ and $CD56^{dim}$ NK cells, which were FACS sorted. Munc13-4 was run on a separate Western blot gel from Stx11 and Munc18-2. Munc13-4 and β-actin for $CD8^+$ T cell and NK cell subsets (rows 1 and 2 in columns 2 and 3) were run on the same Western blot gel as those shown for STAT4 in Figure 5 a (columns 2 and 3) and BRG1 in Figure 5 j (columns 2 and 3), accounting for the shared β-actin image. (b) Cumulative Munc13-4, Stx11, and Munc18-2 fold expression values relative to B cells, naive $CD8^+$ T cells, or $CD56^{bright}$ NK cells from four healthy donors in three independent experiments. All values are normalized to β-actin. Fold expression differences with $P \leq 0.05$ are marked with an asterisk.

protein complex bound to the wild-type *UNC13D* probe that was absent from the probe with the c.118-308C>T mutation. This protein complex migrated at the same size as a probe containing the consensus sequence for the ETS family member ELF1, and addition of an antibody against ELF1 resulted in a super-shift (Fig. 2 d). No super-shifts were observed with antibodies against other ETS family members, including ETS1 and ELF4 (unpublished data).

While examining the *UNC13D* intron 1 region, we identified potential binding sites for several other transcription factors that are associated with effector functions of cytotoxic lymphocytes, including AML/RUNX, NF-κB, and STAT, as well as an evolutionarily conserved transcriptional start site downstream of the ETS site (Fig. 2 c). This led us to hypothesize that the *UNC13D* intron 1 region could represent a lymphocyte-specific alternative promoter. To test this, we performed 5′-RACE on cDNA from primary peripheral blood NK cells and $CD8^+$ T cells using an antisense primer specific for exon 6 of *UNC13D*. This yielded both the conventional *UNC13D* transcript and an additional transcript originating within intron 1 that contained an alternative first exon that is spliced in frame with the downstream coding exons (Fig. 2 e). Corroborating our findings, *UNC13D* transcripts initiating from the intron 1 promoter are present within the NCBI EST dataset (EST CR983520) for lymphocytes, and ELF1 binding to intron 1 is present in ENCODE chromatin immunoprecipitation (ChIP) data for K562 cells (ENCODE Project Consortium, 2011).

To further elucidate the nature of the *UNC13D* intron 1 regulatory element, we designed primers and probes specific for the conventional and intron 1 *UNC13D* transcripts and performed qRT-PCR on sorted $CD19^+$ B cells, $CD4^+$ T cells, $CD8^+$ T cells, $CD3^-CD56^+$ NK cells, and monocytes from healthy donors and an individual homozygous for the *UNC13D* c.118-308C>T mutation. Conventional *UNC13D* transcripts were expressed at comparable levels between subsets in healthy donors and were significantly lower, but still readily detectible, in all analyzed cellular subsets from the individual with the *UNC13D* c.118-308C>T mutation (Fig. 3 a). *UNC13D* transcripts originating from intron 1 were expressed in a lymphocyte–specific pattern in healthy donors, with the highest levels observed in $CD8^+$ T cells and $CD3^-CD56^+$ NK cells. Intron 1 transcripts were observed at the limit of detection in B cells and were not detectable in $CD4^+$ T cells, $CD8^+$ T cells $CD3^-CD56^+$ NK cells, or monocytes from the homozygous *UNC13D* c.118-308C>T patient (Fig. 3 b).

To test the transcriptional activity of the *UNC13D* intron 1 promoter, we created a luciferase reporter vector and tested its activity in the readily transfectable YT-Indy NK cell line. Luciferase expression levels from the intron 1 promoter were comparable to those of the full-length *UNC13D* promoter. We also created a version of the intron 1 promoter reporter vector with the *UNC13D* c.118-308C>T mutation. Remarkably, luciferase levels were not statistically different between the wild-type and mutated versions (Fig. 4 a), suggesting that the ELF1-binding site is not essential for promoter transactivation. Moreover, $CD19^+$ B cells, $CD4^+$ T cells, $CD8^+$ T cells, and $CD3^-CD56^+$ NK cells all expressed similar levels of ELF1 (Fig. 4, b and c). Together, the results suggest that the *UNC13D* intron 1 regulatory element serves as both an enhancer for the conventional promoter and a lymphocyte-specific alternative promoter, and the intronic ELF1 site alone may not explain the observed increase in Munc13-4 expression upon cytotoxic lymphocyte differentiation.

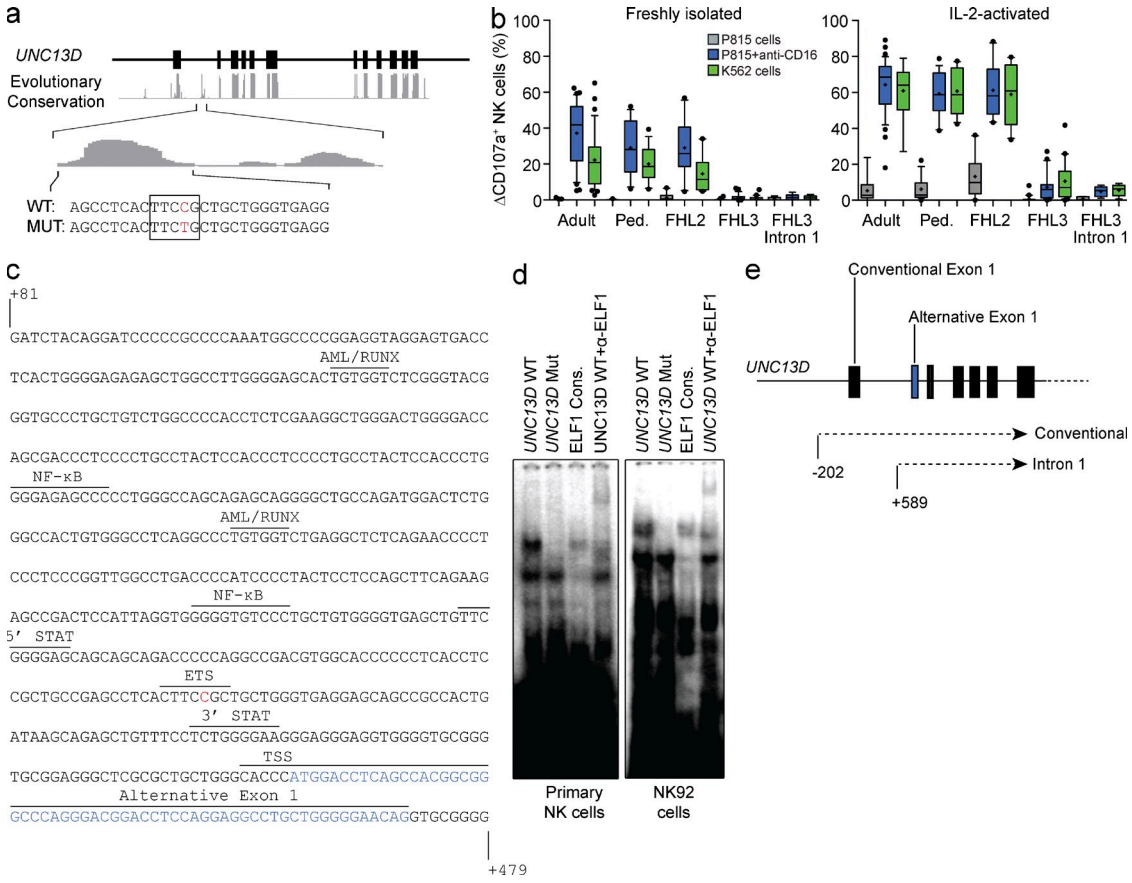

Figure 2. A *UNC13D* c.118-308C>T mutation causative of FHL3 lies within an intronic regulatory element of *UNC13D* and abrogates binding of the transcription factor ELF1. (a) Evolutionary conservation of nucleotides (gray bars) as predicted by the AlaMut algorithm in intronic (black line) and exonic (black boxes) regions of *UNC13D*. The c.118-308C>T mutation is highlighted in red. (b) Freshly isolated and IL-2–stimulated NK cells from 36 healthy adults, 17 healthy children, 10 FHL2 patients, 24 FHL3 patients with bialleic *UNC13D* mutations, and 5 FHL3 patients with bialleic *UNC13D* mutations, of which at least one allele harbored an *UNC13D* intron 1 mutation were stimulated with P815 cells, P815 cells with anti-CD16 antibody, or K562 targets. Degranulation was measured by FACS analysis of CD107a expression on the cell surface. Results represent cumulative data from multiple independent experiments. (c) Nucleotide sequence of intron 1 of *UNC13D*. Predicted transcription factor binding sites are labeled, and the location of the c.118-308C>T mutation is marked in red. Putative alternative transcriptional start site (TSS) and alternative first exon (blue text) are also labeled. (d) EMSA with nuclear lysates from primary NK cells and NK92 cells showing that a protein complex containing ELF1 binds to intron 1 of *UNC13D*, and the c.118-308C>T mutation abrogates binding. Data are representative of three independent experiments with NK cell lysates from two healthy donors and NK92 cells. (e) Location of transcriptional starts relative to the conventional translational start site of *UNC13D* in primary CD56+ NK cells and CD8+ T cells as identified by 5′ RACE in four healthy individuals in four independent experiments.

The ELF1-binding site within intron 1 of *UNC13D* is important for STAT4 recruitment and chromatin remodeling

Because the c.118-308C>T mutation did not significantly affect promoter transactivation in luciferase reporter assays and ELF1 expression levels do not correlate with lymphocyte cytotoxicity, we hypothesized that an intact ELF1-binding site is necessary for the recruitment of additional factors that facilitate the establishment of open chromatin within the *UNC13D* regulatory region, ultimately leading to enhanced Munc13-4 expression. Notably, two potential STAT binding sites are located in close proximity to the ETS consensus site in intron 1 of *UNC13D* (Fig. 2 c). Furthermore, the expression pattern of STAT4 in lymphocyte subsets (Fig. 5, a and b) mirrors that of Munc13-4 (Fig. 1, a and b). To determine whether these putative STAT sites were active, we synthesized probes containing either the STAT site 5′ to the ELF1 site or 3′ to the ELF1 site and tested them in an EMSA with NK92 nuclear protein lysate. A protein complex was clearly visible with the 5′ STAT probe, but not the 3′ STAT probe (Fig. 5 c). To test whether there is interdependence between the ELF1 and 5′ STAT sites, we synthesized 87 bp probes containing either the wild-type or c.118-308C>T mutation along with either the 5′ STAT or 3′ STAT site. In EMSA assays using nuclear lysate from primary NK cells, the presence of a protein complex was evident on the probe with the wild-type ELF1 site and 5′ STAT site, and the c.118-308C>T mutation led to a reduction in binding. No discernable protein complex was observed with probes containing the 3′ STAT site (Fig. 5 d, left). Using nuclear protein from NK92 cells, we also observed the presence of a protein complex on the probe

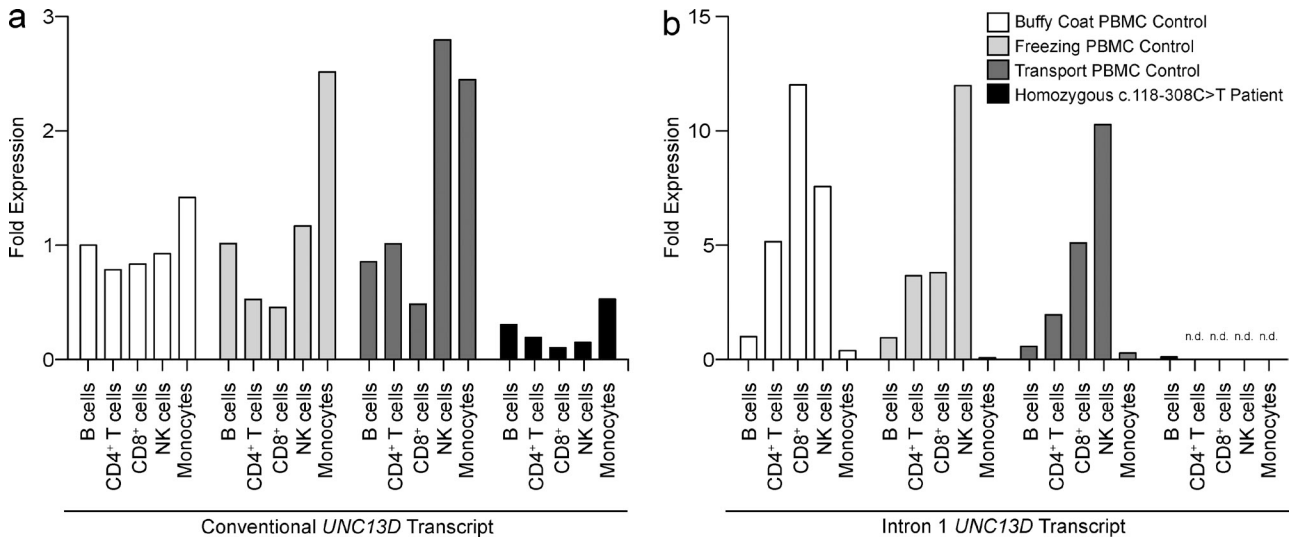

Figure 3. The *UNC13D* intron 1 regulatory element acts as an enhancer and lymphocyte-specific alternative promoter. Quantitative RT-PCR using primers and probes specific for the (a) conventional and (b) intron 1 *UNC13D* transcripts in sorted B cells, CD4+ T cells, CD8+ T cells, NK cells, and monocytes from a fresh, healthy buffy coat donor, healthy donor cells that were previously frozen, healthy donor cells that were frozen and transported, and a homozygous c.118-308C>T patient that were frozen and transported. All PCR data are normalized to 18S RNA levels, and fold expression values were calculated for each donor relative to B cells. All PCRs were performed in triplicate and averaged. All data were generated together in a single experiment with sorted cells from the homozygous donor.

with the wild-type ELF1 site and the 5′ STAT site that was diminished in the presence of the c.118-308C>T mutation. Importantly, binding of the protein complex could be almost entirely competed away with cold probes containing either the consensus ELF1 site or the consensus STAT4 site (Fig. 5 d, right). Binding of the protein complex to the probe could also be inhibited by the addition of an antibody against STAT4 and to a somewhat lesser extent with the addition of an antibody against ELF1 (Fig. 5 d right). The weak effect of the ELF1 antibody in this assay is likely caused by epitope masking by bound STAT4. STAT4 binding to intron 1 of *UNC13D* was confirmed in NK cells by ChIP analysis (Fig. 5 e).

To more definitively demonstrate specificity and determine whether the c.118-308C>T mutation abrogates STAT4 binding to intron 1 of *UNC13D* in the context of native chromatin, we took advantage of linked polymorphisms surrounding the mutation to design PCR primers that specifically amplify the wild-type or mutant *UNC13D* alleles (Fig. 5 f). These primers were used in a ChIP experiment with NK cells from an individual heterozygous for the c.118-308C>T mutation. Using this approach, we could detect STAT4 binding to the wild-type allele, but not to the mutant allele (Fig. 5 g).

Zhang and Boothby (2006) demonstrated that STAT4 recruits the Switch (swi)-sucrose nonfermenter (SNF) component

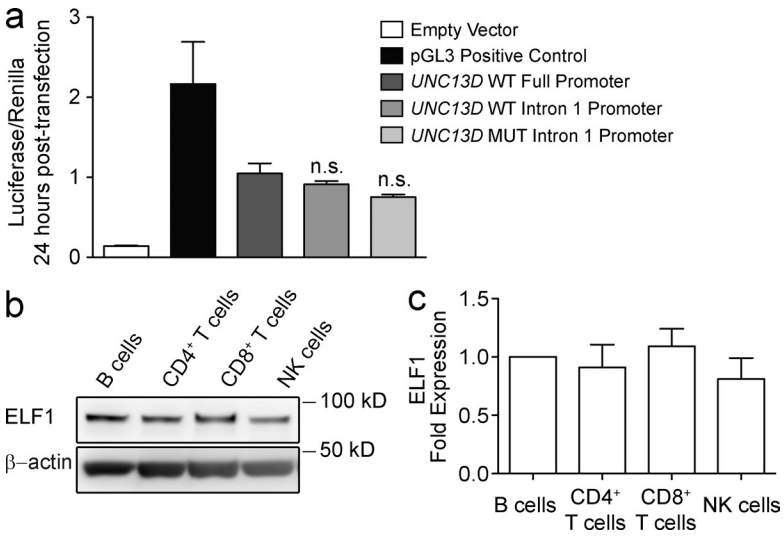

Figure 4. An intact ELF1-binding site is not necessary for active transcription from the regulatory element within intron 1 of *UNC13D*. (a) Luciferase assays showing the relative transcriptional activity of the full *UNC13D* promoter region, the intron 1 promoter region and the intron 1 promoter region with the c.118-308C>T mutation in the YT-Indy NK cell line. Cumulative results from three independent experiments are shown. (b) Western blot analysis of ELF1 expression in isolated subsets of human peripheral blood lymphocytes from a healthy donor. (c) Cumulative ELF1 fold expression values relative to B cells from three donors in two independent experiments. All values are normalized to β-actin.

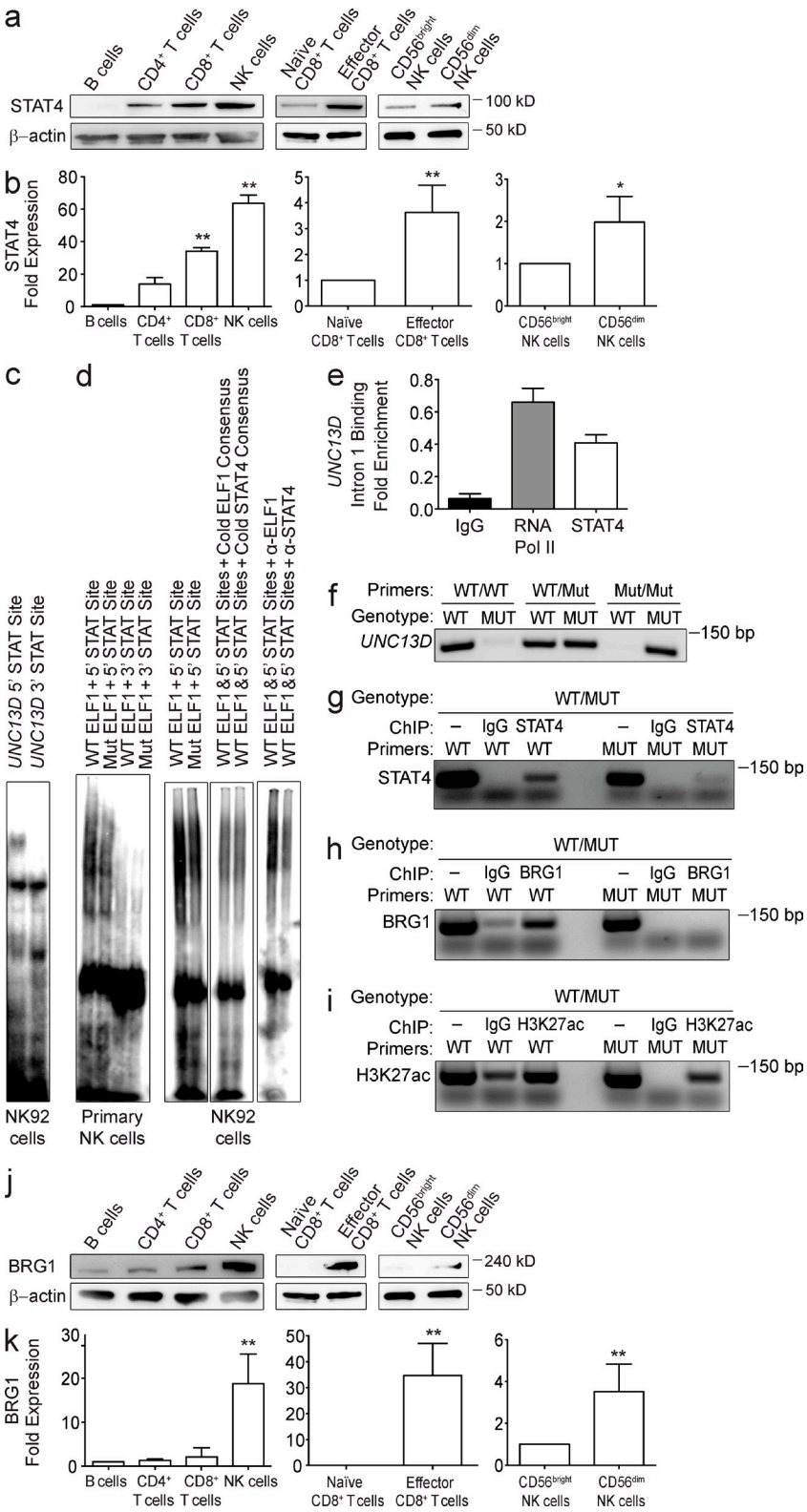

Figure 5. The ELF1-binding site within the *UNC13D* intron 1 regulatory element is important for the recruitment of STAT4, the chromatin remodeling complex BRG1 and high levels of H3K27ac. (a) Western blot analysis of STAT4 expression in isolated subsets of human peripheral blood lymphocytes from a healthy donor. STAT4 and β-actin for $CD8^+$ T cell and NK cell subsets (columns 2 and 3) were run on the same Western blot gel as those shown for Munc13-4 in Fig. 1 a (rows 1 and 2 in columns 2 and 3), accounting for the shared β-actin image. (b) Cumulative STAT4 fold expression values relative to B cells, naive $CD8^+$ T cells or $CD56^{bright}$ NK cells from four donors in three independent experiments. All values are normalized to β-actin. Fold expression differences with $P \leq 0.05$ are marked with a single asterisk, and with $P \leq 0.01$ are marked with a double asterisk. (c) EMSA with probes for the *UNC13D* 5′ and 3′ STAT sites with nuclear lysates from NK92 cells. Data are representative of three independent experiments. (d) EMSA with longer probes spanning the wild-type or mutant ELF1 and 5′ or 3′ STAT sites within intron 1 of *UNC13D* with lysates from primary NK cells (left). EMSA with longer probes spanning the wild-type or mutant ELF1 and 5′ STAT sites with and without cold consensus ELF1- and STAT4-binding sequences or anti-ELF1 and anti-STAT4 antibodies with lysates from NK92 cells (right). All three sections in this figure are from one gel. Data are representative of two independent experiments. (e) ChIP analysis of STAT4 and RNA Pol II binding to intron 1 of *UNC13D*. Cumulative quantitative RT-PCR fold enrichment values relative to input for three separate experiments are shown. (f) Control PCRs showing the specificity of primers used to distinguish between the wild-type and mutant intron 1 regions of *UNC13D* in an individual heterozygous for the c.118-308C>T intron 1 mutation. ChIP analysis of allele-specific (g) STAT4 and (h) BRG1 binding, as well as (i) H3K27ac, in primary NK cells from an individual heterozygous for the c.118-308C>T intron 1 mutation. All data were generated in a single experiment with the heterozygous donor. (j) Western blot analysis of BRG1 expression in isolated subsets of human peripheral blood lymphocytes from a healthy donor. BRG1 and β-actin for $CD8^+$ T cell and NK cell subsets (columns 2 and 3) were run on the same Western blot gel as those shown for Munc13-4 in Fig. 1 a (rows 1 and 2 in columns 2 and 3), accounting for the shared β-actin image. (k) Cumulative BRG1 fold expression values relative to B cells, naive $CD8^+$ T cells, or $CD56^{bright}$ NK cells from four healthy donors in three independent experiments. All values are normalized to β-actin. Fold expression differences with $P \leq 0.01$ are marked with a double asterisk.

Brahma-related gene 1 (BRG1) to the IFN-γ gene in $CD4^+$ T cells undergoing Th1 differentiation. The Swi–SNF remodeling complex uses ATP hydrolysis to slide histone octamers and enhance nucleosomal DNA accessibility, which is a fundamental requirement for transcription (Narlikar et al., 2002). BRG1 recruitment is associated with high levels of H3K27 acetylation on surrounding chromatin (Rada-Iglesias et al., 2011). To determine whether BRG1 is recruited to the

intron 1 promoter of *UNC13D* and is associated with high H3K27ac levels, we performed BRG1 and H3K27ac ChIP analysis with cells from the *UNC13D* heterozygous donor. Using allele-specific primers, we were able to detect BRG1 binding to the wild-type allele, whereas binding was absent on the mutant allele (Fig. 5 h). Similarly, we observed strong enrichment of H3K27ac on the wild-type allele, whereas the mutant allele exhibited reduced levels of H3K27ac (Fig. 5 i). Therefore, an intact ELF1-binding site is necessary for the recruitment of STAT4 and BRG1 and high levels of active chromatin marks within intron 1 of *UNC13D*. Additionally, we analyzed BRG1 expression in lymphocyte subsets and found a strong positive correlation between BRG1 levels and differentiation of cytotoxic lymphocyte subsets (Fig. 5, j and k).

Analysis of the epigenetic landscape of *UNC13D* in primary lymphocyte subsets

To analyze *UNC13D* with high resolution, we designed 24 primer pairs covering a region extending from −2,433 to +12,689 nt relative to the translational start site (Fig. 6 a). These primers were used to identify nucleosome-depleted, open chromatin using the formaldehyde-assisted isolation of regulatory elements (FAIRE) approach (Simon et al., 2012). We observed an enrichment of open chromatin in the conventional and intron 1 promoters in NK cells relative to B cells (Fig. 6 b), which express very low levels of STAT4 (Fig. 5, a and b). Similarly, effector $CD8^+$ T cells displayed an enrichment of open chromatin in the promoter and intron 1 regions relative to naive $CD8^+$ T cells. High-resolution ChIP analysis with an antibody against STAT4 showed that STAT4 (Fig. 6 c) and BRG1 (Fig. 6 d) binding are enriched within intron 1 in NK cells and effector $CD8^+$ T cells. The active histone marks (Karlić et al., 2010) H3K4me3 (Fig. 6 e) and H3K27ac (Fig. 6 f) were enriched throughout the conventional and intron 1 promoters in NK cells and effector $CD8^+$ T cells. Collectively, the ChIP data indicate a poised environment surrounding the first exon of *UNC13D* in all lymphocyte subsets, with an increase in STAT4 and BRG1 binding in NK cells and effector T cells concomitant with increases in active histone marks.

Activation of the TCR signaling pathway induces Munc13-4 expression in $CD8^+$ T cells

Next, we sought to address the question of how signaling may induce Munc13-4 expression. We chose to focus on $CD8^+$ T cells for these experiments due to low basal levels of STAT4 in naive $CD8^+$ T cells and the fact that STAT4 is dramatically up-regulated in effector $CD8^+$ T cells (Fig. 5, a and b), which exhibit strong degranulation, relative to naive $CD8^+$ T cells (Chiang, et al., 2013). To this end, we stimulated naive $CD8^+$ T cells for 16 h with IL-2 and IL-12, IFN-γ, IFN-α, or anti-CD3/CD28 beads and determined Munc13-4, STAT4, phosphorylated STAT4 (pY693; pSTAT4), and BRG1 protein expression levels by Western blot. Cytokine stimulation alone did not induce expression of any of these proteins. However, CD3/CD28 stimulation robustly increased the expression of all three proteins along with robust pSTAT4 (Fig. 7, a and b). Phosphorylation on tyrosine 693 is important for STAT4 transcriptional activity (Visconti et al., 2000). Of note, we observed an approximately threefold induction of both conventional and alternative intron 1 transcripts in CD3/CD28-stimulated cells (unpublished data).

To more accurately delineate relative temporal expression patterns, we stimulated naive $CD8^+$ T cells with CD3/CD28 beads for 2, 4, 8, or 16 h and performed Western blots. We observed rapid induction of BRG1 between 2 and 4 h, followed by STAT4 induction between 4 and 8 h. Significant Munc13-4 induction was observed between 8 and 16 h (Fig. 7, c and d). Thus, antigen receptor stimulation is sufficient to induce expression of all three proteins, with more rapid kinetics observed for BRG1 and STAT4. To determine whether STAT4 is activated before Munc13-4 induction, we stimulated naive $CD8^+$ T cells with CD3/CD28 beads for 0.5, 1, 2, 4, 6, 8, 12, or 16 h and performed Western blots for total and phosphorylated STAT4. Induction of pSTAT4 was consistently observed between 2 and 4 h and increased over time, with a peak at 12 h after stimulation (Fig. 7, e and f). Therefore, STAT4 phosphorylation precedes Munc13-4 induction in naive $CD8^+$ T cells upon engagement of the TCR signaling pathway and could thus promote Munc13-4 expression upon T cell activation.

STAT4 is required for Munc13-4 induction upon TCR signaling

To establish a direct link between STAT4 and the induction of Munc13-4 expression after TCR stimulation, naive $CD8^+$ T cells were isolated from peripheral blood and transfected with either control siRNA or siRNA-targeting STAT4 (siSTAT4). Upon CD3/CD28 stimulation, STAT4 was highly induced in cells transfected with the control siRNA. No STAT4 induction was observed in cells transfected with siSTAT4, confirming the efficacy of the knockdown. As expected, Munc13-4 was induced upon stimulation in cells transfected with control siRNA. Notably, Munc13-4 protein levels were 76 ± 12% lower in siSTAT4-transfected cells compared with siRNA controls, supporting the hypothesis that STAT4 is important for Munc13-4 induction. BRG1 was comparably induced in both control and siSTAT4 transfected cells, suggesting that TCR signaling induces BRG1 expression independent of STAT4 (Fig. 8, a and b). These results provide conclusive evidence demonstrating a significant role for STAT4 in the regulation of Munc13-4 expression.

DISCUSSION

By studying a mutation that causes specific defects in lymphocyte cytotoxicity, we have delineated a critical role for STAT4 in regulating Munc13-4 expression upon cytotoxic lymphocyte differentiation and identified a novel, evolutionarily conserved promoter within intron 1 of *UNC13D*. The intronic c.118-308C>T mutation causative of FHL3 abolished an ELF1-binding site that is necessary for the recruitment of STAT4 and BRG1 as well as the acquisition of histone marks permissive for transcription. TCR stimulation

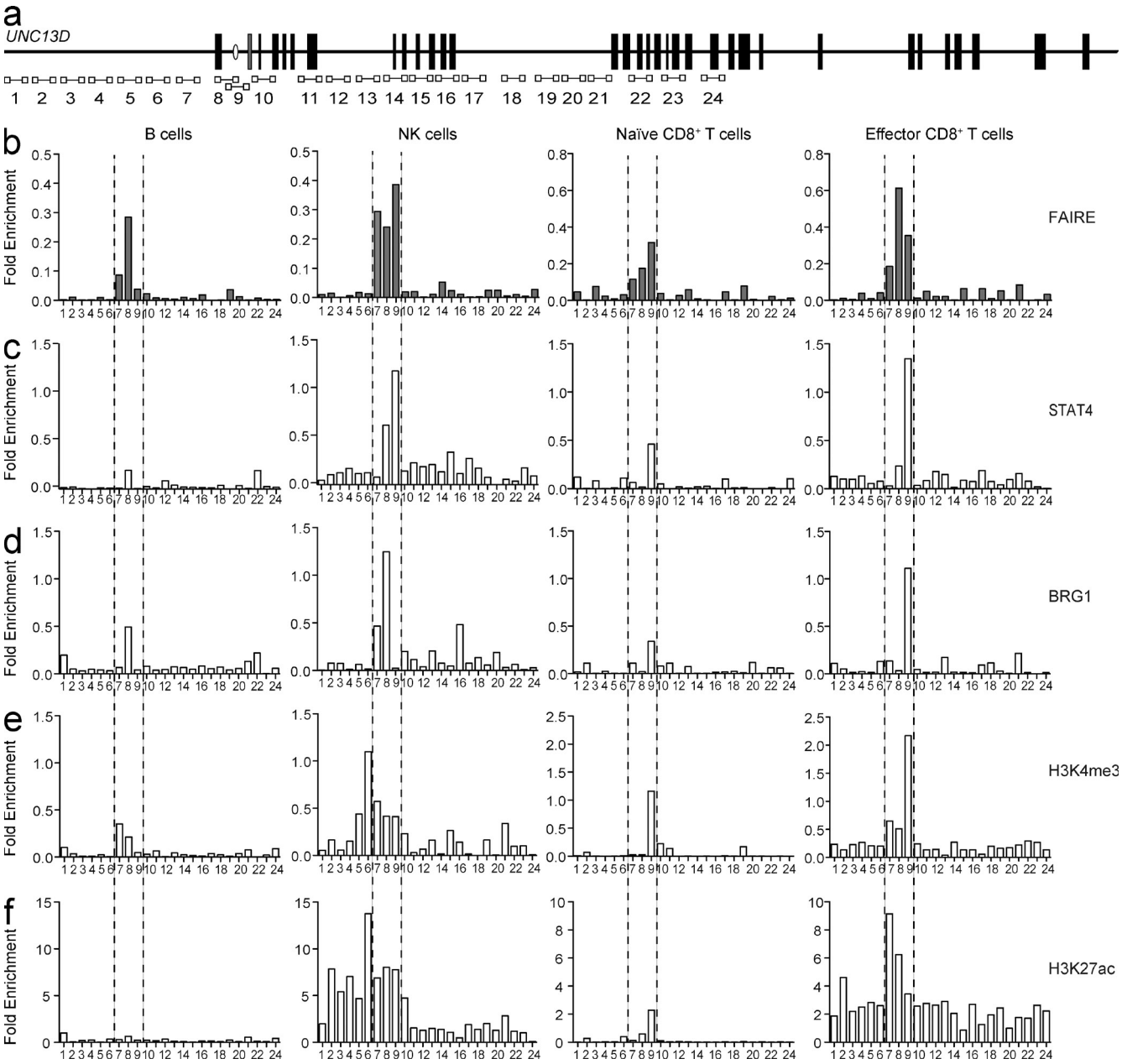

Figure 6. High-resolution comparison of the *UNC13D* chromatin state in lymphocyte subsets. (a) Locations of primer pairs that were used for high-resolution analysis of *UNC13D*. The primers map a region spanning from −2,433 to +12,689 (relative to the conventional translational start site), and each primer pair was designed to amplify a 150–200-bp product. The location of the ELF1-binding site is indicated with an open circle. The alternative first exon is labeled in blue. (b) FAIRE analysis of open chromatin in primary B, NK, $CD8^+$ naïve, and $CD8^+$ effector T cells. Quantitative RT-PCR values averaged from two donors in two independent experiments are shown. (c–f) ChIP assays with antibodies against STAT4, BRG1, H3K4me3, and H3K27ac. Expression values normalized to an IgG-negative control and to input are shown. Quantitative RT-PCR values averaged from two donors in two independent experiments are shown.

of naive $CD8^+$ T cells led to robust induction of Munc13-4, STAT4, and BRG1, and knockdown of STAT4 abrogated induction of Munc13-4 expression. Our data show that the *UNC13D* intronic sequence can act both as an alternative promoter and as a general enhancer, promoting Munc13-4 expression upon cytotoxic lymphocyte differentiation.

A surprising finding from our analysis of lymphocyte subsets was that Munc13-4 expression levels are selectively upregulated upon cytotoxic lymphocyte differentiation. Feldmann et al. (2003) reported similar levels of *UNC13D* mRNA transcripts by conventional RT-PCR analysis in all hematopoietic cells analyzed including $CD4^+$ and $CD8^+$ T cells and $CD19^+$

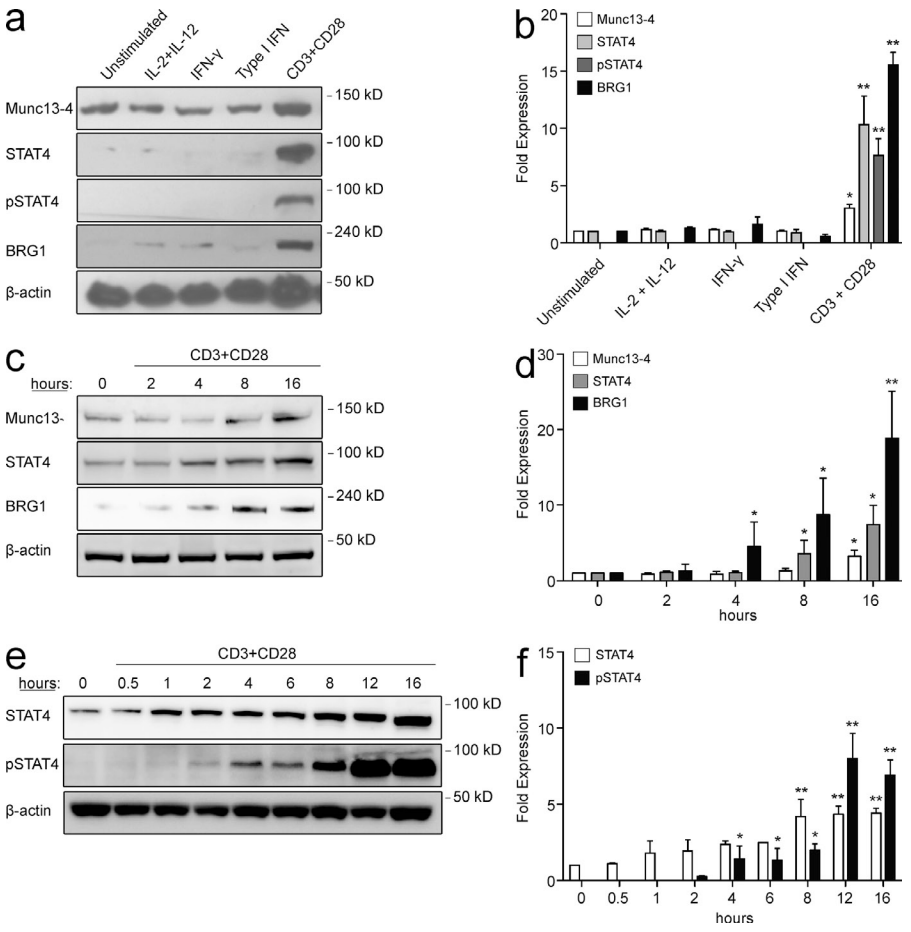

Figure 7. CD3–CD28 signaling induces Munc13-4, STAT4, and BRG1 expression in naive CD8⁺ T cells. (a) Representative Western blots for Munc13-4, STAT4, pSTAT4, and BRG1 in naive CD8⁺ T cells from a healthy donor stimulated with IL-2 and IL-12, IFN-γ, type I IFN, or anti-CD3/CD28 microbeads. (b) Cumulative Munc13-4, STAT4, pSTAT4, and BRG1 fold expression values from each stimulation condition relative to unstimulated cells from five healthy donors in three independent experiments. All values are normalized to β-actin. (c) Representative Western blots for Munc13-4, STAT4 and BRG1 in naive CD8⁺ T cells from a healthy individual stimulated with anti-CD3/CD28 microbeads for 0, 2, 4, 8, and 16 h. (d) Cumulative Munc13-4, STAT4, and BRG1 fold expression values from each stimulation time point relative to unstimulated cells from three healthy individuals in two independent experiments. All values are normalized to β-actin. (e) Representative Western blots for total and phosphorylated (pY693) STAT4 expression in naive CD8⁺ T cells from a healthy donor at the indicated time points after stimulation with anti-CD3/CD28 microbeads. (f) Cumulative STAT4 and pSTAT4 fold expression values from each stimulation time point relative to unstimulated cells from three healthy donors in two independent experiments. All values are normalized to β-actin. Fold expression differences with $P \leq 0.05$ are marked with a single asterisk, and with $P \leq 0.01$ are marked with a double asterisk.

B cells, but did not explore expression in well-defined naive and cytotoxic subsets. Given that Munc13-4 protein levels closely correlate with degranulative and cytotoxic potential (Chiang et al., 2013), it is likely that Munc13-4 expression represents a critical rate-limiting step for cytotoxic lymphocyte degranulation, as previously shown for platelets (Shirakawa et al., 2004).

The ability of a cell to respond to environmental stimuli and appropriately alter gene expression is a fundamental component

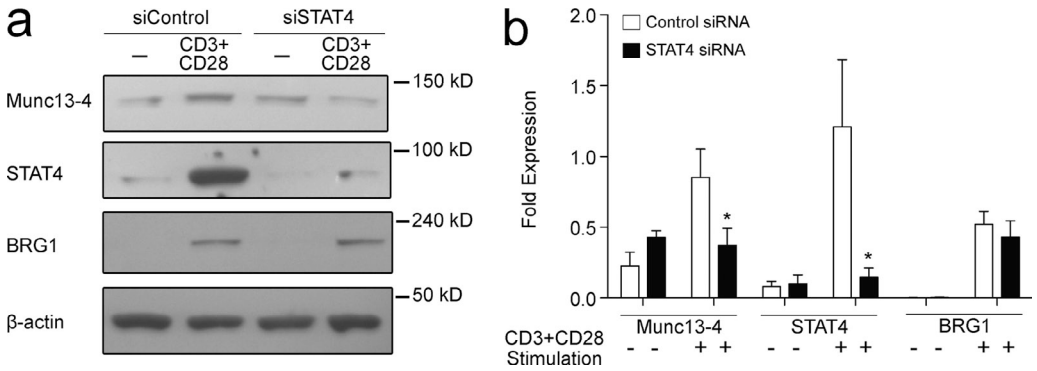

Figure 8. STAT4 is necessary for Munc13-4 induction in response to CD3/CD28 stimulation. (a) Naive CD8⁺ T cells from a healthy donor were transfected with control siRNA or siRNA targeting STAT4 and stimulated overnight with anti-CD3/CD28 microbeads or left unstimulated. Western blots were performed with antibodies against Munc13-4, STAT4, and BRG1. (b) Cumulative Munc13-4, STAT4, and BRG1 fold expression values normalized to β-actin from control siRNA and siSTAT4 transfection and stimulation experiments from four healthy donors in two independent experiments. Fold expression differences between control and STAT4 knockdown conditions with $P \leq 0.05$ are marked with an asterisk.

of evolutionary adaptation. The activation or repression of cell-type-specific gene expression programs takes place at the level of chromatin and is influenced by regulatory elements such as enhancers. The c.118-308C>T mutation causative of FHL3 abolished an ELF1-binding site. ELF1 was expressed at uniform high levels in disparate lymphocyte subsets and did not correlate with expression of Munc13-4, suggesting that other transcription factors might be implicated in induction of Munc13-4 expression upon differentiation. A series of elegant experiments by Vahedi et al. (2012) identified STATs, particularly STAT1 and STAT4, as predominant players in shaping the active global enhancer landscape during $CD4^+$ T cell fate specification. Interestingly, phenotype-defining master regulators such as T-bet had only a modest impact upon the active enhancer landscape.

Our data demonstrate that STAT4 can bind upstream of the ELF1-binding site and that the c.118-308C>T mutation interferes with STAT4 recruitment to intron 1 of *UNC13D*. A strong case can be made for STAT4 as a central transcriptional regulator of effector function in cytotoxic lymphocytes, as it also regulates the expression of perforin (Yamamoto et al., 2002), IFN-γ (Zhang and Boothby, 2006), IL-12R (Letimier et al., 2007), T-bet (Yang et al., 2007), and type 1 IFN (Miyagi et al., 2007). During mouse T_H1 cell differentiation, STAT4 and BRG1 act together in regulation of the *Ifng* promoter (Zhang and Boothby, 2006) and *Il12rb2* enhancer (Letimier et al., 2007). On a genome-wide scale, STAT4 appears to facilitate T_H1 cell differentiation by promoting the acquisition of active epigenetic marks, particularly tri-methylation of lysine 4 on histone 3, at intergenic and promoter-associated binding sites (Wei et al., 2010). We show that STAT4 plays a similar role in altering the epigenetic state of *UNC13D* to allow for transcriptional activation in NK cells and $CD8^+$ T cells. The requirement for STAT4 in *UNC13D* transcriptional regulation may provide an explanation for defective cytotoxicity observed in STAT4-deficient mice (Kaplan et al., 1996). Therefore, STAT4 also represents a driver of epigenetic programming required for degranulation by cytotoxic lymphocytes.

Whether STAT4 directly interacts with ELF1 is also an open question. In a study by Serdobova et al. (1997), ELF1 was shown to bind cooperatively, but not directly, with STAT5 to an IL-2–responsive enhancer in mouse *Il2ra*. Our data demonstrates that a similar cooperative interaction between ELF1 and STAT4 occurs within intron 1 of *UNC13D*. Furthermore, two mechanisms have been identified for the recruitment of BRG1 and the associated Swi–SNF complex to regions of regulatory DNA. In a model proposed by Hassan et al. (2001), retention of SWI–SNF is mediated by histone acetyltransferase (HAT) complexes and acetylated histones. The second mechanism for BRG1 recruitment is through interactions with transcription factors. STAT2, which displays 42% homology amino acid to STAT4, has been shown to directly interact with BRG1 in cell lines (Huang et al., 2002). However, we were not able to detect a direct interaction between STAT4 and BRG1 in primary human NK cells (unpublished data).

Although our experiments have focused on the role of STAT4 in regulation of Munc13-4 expression and shown that knockdown of STAT4 can reduce the TCR-induced up-regulation of Munc13-4 expression by 76% compared with siRNA controls (Fig. 8, a and b), other STAT family members may well contribute to transcriptional regulation of *UNC13D*. ENCODE ChIP-seq data show binding peaks for STAT1, STAT2, STAT3, and STAT5A within intron 1 and the proximal *UNC13D* promoter in IFN-α–stimulated K562 cells (ENCODE Project Consortium, 2011). ChIP-seq analysis for STAT4 binding is not available within this dataset. The binding of each individual STAT member to the *UNC13D* locus in primary cytotoxic lymphocytes and their functional significance will require a more extensive analysis.

Our results demonstrate a direct role for STAT4 in regulating genes required for lymphocyte cytotoxicity downstream of TCR engagement in naive $CD8^+$ T cells. This finding is supported by in vitro TCR stimulation experiments with $CD4^+$ T cells (Bacon et al., 1995) and a recent in vivo study of $CD8^+$ T cell activation by lymphocytic choriomeningitis virus (LCMV) infection in the mouse where stimulation through the TCR induced elevated STAT4 expression and was important for antigen-specific proliferation and activation (Gil et al., 2012). The link between STAT4 and Munc13-4 may have implications in the study of diseases that have been linked to STAT4 polymorphisms. A genetic variant of the *STAT4* locus that results in reduced levels of *STAT4* mRNA expression is associated with an increased risk of hepatitis B virus-related hepatocellular carcinoma (Jiang et al., 2013). Association studies have also identified *STAT4* as a genetic risk factor for rheumatoid arthritis (RA), systemic lupus erythematosus (SLE), and Sjögren's syndrome. The genetic associations with *STAT4* involve SNP variants located within the gene's third intron. Despite clear clinical associations between *STAT4* polymorphisms and autoimmunity, a mechanistic explanation for the role of STAT4 is lacking (Remmers et al., 2007; Korman et al., 2008). The identification of STAT4 targets critical for cytotoxic lymphocyte function, such as *UNC13D*, may be relevant in the context of complex autoimmune syndromes.

Remarkably, our data also revealed that the *UNC13D* c.118-308C>T mutation specifically abrogates transcription of an alternative form of Munc13-4 in lymphocytes. Residual transcripts of the conventional Munc13-4 isoform appear not to be sufficient for supporting any cytotoxic lymphocyte degranulation. The predicted alternative Munc13-4 protein has a unique amino acid sequence at the amino terminus and is 19 amino acids shorter than the conventional Munc13-4 protein. To our knowledge, no disease causing *UNC13D* mutations have hitherto been reported in the conventional first coding exon of *UNC13D*. Thus, it is possible that the alternative, lymphocyte-specific isoform rather than the conventional isoform of Munc13-4 is critical for lymphocyte cytotoxicity. It is therefore of high interest to study the trafficking and function of this alternative Munc13-4 isoform in the setting of cytotoxic lymphocyte degranulation.

In conclusion, the results of this study provide novel insights into the regulatory networks that control lymphocyte cytotoxic function and explain different *UNC13D* intron 1 mutations that represent a frequent cause of FHL3 (Meeths et al., 2011; Entesarian et al., 2013; Seo et al., 2013). Specific mutations that interrupt immune transcription factor binding within cis-regulatory elements likely represent a mechanism causative of many known primary immunodeficiencies, as well as other immune diseases, warranting further investigation.

MATERIALS AND METHODS

Patients and controls. FHL patients were included in this study, as were individuals with monoallelic mutations and/or polymorphisms in *UNC13D*. The patients have been previously described (Meeths et al., 2011). The regional ethics committee at Karolinska Institutet approved this study, and written consent was obtained from all participants.

Cell isolations. Peripheral blood mononuclear cells were freshly isolated from buffy coats by density gradient centrifugation. Untouched lymphocyte subsets were further isolated by negative magnetic bead selection (Miltenyi Biotec or STEMCELL Technologies, Inc.). $CD19^+$ B cells, $CD4^+$ T cells, $CD8^+$ T cells, CD3-$CD56^+$ NK cells, monocytes, $CD56^{bright}$ NK cells, and $CD56^{dim}$ NK cells were isolated by cell sorting (FACSAria; BD) in some experiments.

Flow cytometry. Cells were stained with fluorochrome-conjugated antibodies and incubated for 30 min on ice. The following antibodies were used for labeling cells before sorting: CD56 PE-Cy7 (BD), CD3 PE-Cy5.5 (Invitrogen), CD19 APC-Cy7 (BD), CD8 QDot 705 (Invitrogen), CD45 QDot 655 (Invitrogen), and CD57 Pacific Blue (BioLegend). Cells were sorted with a FACSAria II (BD).

Western blots. Cells were lysed on ice for 30 min in lysis buffer (20 mM Tris-HCl, 150 mM NaCl, 1% Triton-X 100, 2 mM EDTA, 0.2% SDS, and complete protease inhibitor (Roche). Protein lysates were quantified with Bradford analysis (Thermo Fisher Scientific), and 10 µg of each lysate was separated through SDS-PAGE gel electrophoresis (Invitrogen). Protein was then transferred onto Immobilon Transfer Membranes (EMD Millipore) through the fast semi-dry transfer method (Thermo Fisher Scientific). Membranes were stained with anti–Munc13-4, anti–Munc18-2, anti-syntaxin 11 (Proteintech), anti-STAT4, anti-pSTAT4 (Abcam), anti-BRG1 (Abcam), anti-ELF1 (Santa Cruz Biotechnology, Inc.), or anti–β-actin (Sigma-Aldrich) primary antibodies. Secondary staining was performed with anti–rabbit or anti–mouse antibodies conjugated to horseradish peroxidase (Invitrogen). Chemiluminescence was visualized with an ImageQuant LAS 4000 Mini (GE Healthcare), and densitometry values were quantified with ImageJ software (National Institutes of Health).

Electrophoretic mobility shift assays (EMSA). Nuclear extracts were prepared from NK92 cells using the CellLytic NuCLEAR extraction kit (Sigma-Aldrich). Protein concentration was measured with a Bio-Rad protein assay, and samples were stored at −70°C until use. The following DNA oligonucleotide probes were synthesized: UNC13D intron 1 WT/Mut ETS probes AGCCTCACTTC(C/T)GCTGCTGGGTGAGG; UNC13D intron 1 5′ STAT site probe GTGGGGTGAGCTGTTCGGGGAGCAGCAGAC; UNC13D intron 1 3′ STAT site probe GAGCTGTTTCCTCTGGGGAAGGGAGCG; UNC13D intron 1 WT/Mut ETS + 5′ STAT site long probes GTGAGCTGTTCGGGGAGCAGCAGACCCCCAGGCCGACGTGGCACCCCCCTCACCTCCGCTGCCGAGCCTCACTTC(C/T)GCTGCTGGCTC. Probes were labeled with α-[^{32}P]deoxycytidine triphosphate (3000 Ci/mmol; PerkinElmer Life and Analytical Sciences) by fill-in using the Klenow fragment of DNA polymerase I (Invitrogen). [^{32}P]-labeled double-stranded oligonucleotides were purified using mini Quick Spin Oligo Columns (Roche). DNA–protein binding reactions were performed in a 10-µl mixture containing 5 µg nuclear protein and 1 µg poly(dI-dC; Sigma-Aldrich) in 4% glycerol, 1 mM $MgCl_2$, 0.5 mM ethylenediaminetetraacetic acid, 0.5 mM dithiothreitol, 50 mM NaCl, 10 mM Tris-HCl (pH 7.5). Nuclear extracts were incubated with 1 µl ^{32}P-labeled oligonucleotide probe (10,000 cpm) at room temperature for 20 min and then loaded on a 5% polyacrylamide gel (37:5:1). Electrophoresis was performed in 0.5x TBE for 2 h at 130 V, and the gel was visualized by autoradiography.

UNC13D 5′ Rapid Amplification of cDNA Ends (RACE). RNA was isolated from primary $CD56^+$ NK cells and $CD8^+$ T cells from the peripheral blood of healthy donors, and 5′ RACE was performed with the 5′/3′ RACE kit, second generation (Roche) using primers listed in Table S1.

UNC13D promoter luciferase reporter assays. pGL3 (Promega) luciferase reporter constructs were created by PCR using the USER cloning system (NEB) for the *UNC13D* intron 1 promoter region (+5 to +607). A version of the intron 1 promoter with the c.118-308C>T mutation and a full-length version of the *UNC13D* promoter (−1,374 to +607) were also created by USER cloning. Primer sequences are provided in Table S1. These constructs, along with a $pGL3^+$ control, were tested for activity in the YT-INDY NK cell line using the dual luciferase kit (Promega). Analysis was performed on a VICTOR^2 1420 multilabel counter (PerkinElmer). Cells were co-transfected with a renilla plasmid for normalization measurements. Nucleofections were performed using the Amaxa Human Monocyte Nucleofector kit (Lonza) using the Y-10 program.

ChIP assays. Primary human peripheral blood NK cells or B cells were cross-linked with 1% formaldehyde and sheared with a Misonix sonicator. For each sample, 10^6 cell equivalents of chromatin were immunoprecipitated with the EZ-ChIP chromatin immunoprecipitation kit (Millipore) using 1 µg each of the following ChIP-grade antibodies: mouse IgG (Millipore), RNA polymerase II (Millipore), STAT4 (Abcam), anti-histone H3 (acetyl K27; Abcam), anti-BRG1 (Abcam), and anti-histone H3 (tri-methyl K4; Abcam). Cross-links were reversed by incubation at 65°C with the addition of proteinase K overnight.

Formaldehyde-assisted identification of regulatory elements (FAIRE). Primary human peripheral blood NK cells or B cells were cross-linked with 1% formaldehyde and sheared with a Misonix sonicator. Input and phenol chloroform-extracted DNA was isolated from 5×10^6 cell equivalents of chromatin according to published methods (Simon et al., 2012), and open chromatin was assessed by qRT-PCR.

PCR and quantitative real-time PCR. PCR was performed using Platinum Taq DNA Polymerase (Invitrogen) with 35 cycles of the following incubations: 94°C for 20 s, 60°C for 30 s, and 72°C for 1 min. Quantitative real-time PCR was performed using SYBR Green or TaqMan reagents (QIAGEN) on a 7500 real time PCR system (Applied Biosystems). All primer sequences are provided in Table S1.

Naive T cell stimulations. Naive $CD8^+$ T cells were isolated from the peripheral blood of healthy donors. 2×10^6 cells were cultured overnight in the following conditions: no stimulation, 200 U/ml IL-2 (PeproTech) plus 10 ng/ml IL-12 (PeproTech), 1 ng/ml IFN-γ (R&D Systems), 1 U/ml IFN-α (PBL), or 75 µl/ml CD3/CD28 microbeads (Life Technologies).

siRNA transfections. 3×10^6 naive $CD8^+$ T cells were transfected with 40 pmol control siRNA or siRNA targeting STAT4 (QIAGEN) using the Amaxa Human T Cell Nucleofector kit (Lonza). The U-014 Nucleofector program was used for high cell viability.

Statistical methods. Statistical significance was determined by paired Student's *t* tests using GraphPad software.

Online supplemental material. Table S1 shows custom *UNC13D* primers. Online supplemental material is available at http://www.jem.org/cgi/content/full/jem.20131131/DC1.

This work was supported by the European Research Council under the European Union's Seventh Framework Program (FP/2007-2013)/ERC Grant Agreement n. 311335, Swedish Research Council, Swedish Foundation for Strategic Research, Swedish Cancer Foundation, Swedish Children's Cancer Foundation, Histiocytosis Association, Jeansson's Foundation, Åke Wiberg's Foundation, the Karolinska Institute Research Foundation, the Frontiers in Biomedical Research Fellowship, and University of Minnesota T32 Haematology Training Grant. This project has been funded in whole or in part with Federal funds from the Frederick National Laboratory for Cancer Research, National Institutes of Health, under contract HHSN261200800001E. This research was supported in part by the Intramural Research Program of National Institutes of Health, Frederick National Laboratory, Center for Cancer Research. The content of this publication does not necessarily reflect the views or policies of the Department of Health and Human Services, nor does mention of trade names, commercial products, or organizations imply endorsement by the US Government.

The authors have no conflicting financial interests.

Submitted: 31 May 2013
Accepted: 11 April 2014

REFERENCES

Bacon, C.M., E.F. Petricoin III, J.R. Ortaldo, R.C. Rees, A.C. Larner, J.A. Johnston, and J.J. O'Shea. 1995. Interleukin 12 induces tyrosine phosphorylation and activation of STAT4 in human lymphocytes. *Proc. Natl. Acad. Sci. USA*. 92:7307–7311. http://dx.doi.org/10.1073/pnas.92.16.7307

Brennan, A.J., J. Chia, J.A. Trapani, and I. Voskoboinik. 2010. Perforin deficiency and susceptibility to cancer. *Cell Death Differ.* 17:607–615. http://dx.doi.org/10.1038/cdd.2009.212

Casanova, J.L., and L. Abel. 2004. The human model: a genetic dissection of immunity to infection in natural conditions. *Nat. Rev. Immunol.* 4:55–66. http://dx.doi.org/10.1038/nri1264

Chiang, S.C., J. Theorell, M. Entesarian, M. Meeths, M. Mastafa, W. Al-Herz, P. Frisk, K.C. Gilmour, M. Ifversen, C. Langenskiöld, et al. 2013. Comparison of primary human cytotoxic T-cell and natural killer cell responses reveal similar molecular requirements for lytic granule exocytosis but differences in cytokine production. *Blood*. 121:1345–1356. http://dx.doi.org/10.1182/blood-2012-07-442558

de Saint Basile, G., G. Ménasché, and A. Fischer. 2010. Molecular mechanisms of biogenesis and exocytosis of cytotoxic granules. *Nat. Rev. Immunol.* 10:568–579. http://dx.doi.org/10.1038/nri2803

ENCODE Project Consortium. 2011. A user's guide to the encyclopedia of DNA elements (ENCODE). *PLoS Biol.* 9:e1001046. http://dx.doi.org/10.1371/journal.pbio.1001046

Entesarian, M., S.C. Chiang, H. Schlums, M. Meeths, M.Y. Chan, S.N. Mya, S.Y. Soh, M. Nordenskjöld, J.I. Henter, and Y.T. Bryceson. 2013. Novel deep intronic and missense UNC13D mutations in familial haemophagocytic lymphohistiocytosis type 3. *Br. J. Haematol.* 162:415–418. http://dx.doi.org/10.1111/bjh.12371

Feldmann, J., I. Callebaut, G. Raposo, S. Certain, D. Bacq, C. Dumont, N. Lambert, M. Ouachée-Chardin, G. Chedeville, H. Tamary, et al. 2003. Munc13-4 is essential for cytolytic granules fusion and is mutated in a form of familial hemophagocytic lymphohistiocytosis (FHL3). *Cell*. 115:461–473. http://dx.doi.org/10.1016/S0092-8674(03)00855-9

Fratkin, E., S. Bercovici, and D.A. Stephan. 2012. The implications of ENCODE for diagnostics. *Nat. Biotechnol.* 30:1064–1065. http://dx.doi.org/10.1038/nbt.2418

Gil, M.P., M.J. Ploquin, W.T. Watford, S.H. Lee, K. Kim, X. Wang, Y. Kanno, J.J. O'Shea, and C.A. Biron. 2012. Regulating type 1 IFN effects in CD8 T cells during viral infections: changing STAT4 and STAT1 expression for function. *Blood*. 120:3718–3728. http://dx.doi.org/10.1182/blood-2012-05-428672

Hassan, A.H., K.E. Neely, and J.L. Workman. 2001. Histone acetyltransferase complexes stabilize swi/snf binding to promoter nucleosomes. *Cell*. 104:817–827. http://dx.doi.org/10.1016/S0092-8674(01)00279-3

Heinemeyer, T., E. Wingender, I. Reuter, H. Hermjakob, A.E. Kel, O.V. Kel, E.V. Ignatieva, E.A. Ananko, O.A. Podkolodnaya, F.A. Kolpakov, et al. 1998. Databases on transcriptional regulation: TRANSFAC, TRRD and COMPEL. *Nucleic Acids Res.* 26:362–367. http://dx.doi.org/10.1093/nar/26.1.362

Huang, M., F. Qian, Y. Hu, C. Ang, Z. Li, and Z. Wen. 2002. Chromatin-remodelling factor BRG1 selectively activates a subset of interferon-alpha-inducible genes. *Nat. Cell Biol.* 4:774–781. http://dx.doi.org/10.1038/ncb855

Janka, G.E. 2012. Familial and acquired hemophagocytic lymphohistiocytosis. *Annu. Rev. Med.* 63:233–246. http://dx.doi.org/10.1146/annurev-med-041610-134208

Jiang, D.K., J. Sun, G. Cao, Y. Liu, D. Lin, Y.Z. Gao, W.H. Ren, X.D. Long, H. Zhang, X.P. Ma, et al. 2013. Genetic variants in STAT4 and HLA-DQ genes confer risk of hepatitis B virus-related hepatocellular carcinoma. *Nat. Genet.* 45:72–75. http://dx.doi.org/10.1038/ng.2483

Kaplan, M.H., Y.L. Sun, T. Hoey, and M.J. Grusby. 1996. Impaired IL-12 responses and enhanced development of Th2 cells in Stat4-deficient mice. *Nature*. 382:174–177. http://dx.doi.org/10.1038/382174a0

Karlić, R., H.R. Chung, J. Lasserre, K. Vlahovicek, and M. Vingron. 2010. Histone modification levels are predictive for gene expression. *Proc. Natl. Acad. Sci. USA*. 107:2926–2931. http://dx.doi.org/10.1073/pnas.0909344107

Koch, H., K. Hofmann, and N. Brose. 2000. Definition of Munc13-homology-domains and characterization of a novel ubiquitously expressed Munc13 isoform. *Biochem. J.* 349:247–253. http://dx.doi.org/10.1042/0264-6021:3490247

Korman, B.D., M.I. Alba, J.M. Le, I. Alevizos, J.A. Smith, N.P. Nikolov, D.L. Kastner, E.F. Remmers, and G.G. Illei. 2008. Variant form of STAT4 is associated with primary Sjögren's syndrome. *Genes Immun.* 9:267–270. http://dx.doi.org/10.1038/gene.2008.1

Letimier, F.A., N. Passini, S. Gasparian, E. Bianchi, and L. Rogge. 2007. Chromatin remodeling by the SWI/SNF-like BAF complex and STAT4 activation synergistically induce IL-12Rbeta2 expression during human Th1 cell differentiation. *EMBO J.* 26:1292–1302. http://dx.doi.org/10.1038/sj.emboj.7601586

Meeths, M., S.C. Chiang, S.M. Wood, M. Entesarian, H. Schlums, B. Bang, E. Nordenskjöld, C. Björklund, G. Jakovljevic, J. Jazbec, et al. 2011. Familial hemophagocytic lymphohistiocytosis type 3 (FHL3) caused by deep intronic mutation and inversion in UNC13D. *Blood*. 118:5783–5793. http://dx.doi.org/10.1182/blood-2011-07-369090

Ménager, M.M., G. Ménasché, M. Romao, P. Knapnougel, C.H. Ho, M. Garfa, G. Raposo, J. Feldmann, A. Fischer, and G. de Saint Basile. 2007. Secretory cytotoxic granule maturation and exocytosis require the effector protein hMunc13-4. *Nat. Immunol.* 8:257–267. http://dx.doi.org/10.1038/ni1431

Miyagi, T., M.P. Gill, X. Wang, J. Louten, W.M. Chu, and C.A. Biron. 2007. High basal STAT4 balanced by STAT1 induction to control type 1 interferon effects in natural killer cells. *J. Exp. Med.* 204:2383–2396.

Narlikar, G.J., H.Y. Fan, and R.E. Kingston. 2002. Cooperation between complexes that regulate chromatin structure and transcription. *Cell*. 108:475–487. http://dx.doi.org/10.1016/S0092-8674(02)00654-2

Rada-Iglesias, A., R. Bajpai, T. Swigut, S.A. Brugmann, R.A. Flynn, and J. Wysocka. 2011. A unique chromatin signature uncovers early developmental enhancers in humans. *Nature*. 470:279–283. http://dx.doi.org/10.1038/nature09692

Remmers, E.F., R.M. Plenge, A.T. Lee, R.R. Graham, G. Hom, T.W. Behrens, P.I. de Bakker, J.M. Le, H.S. Lee, F. Batliwalla, et al. 2007. STAT4 and the risk of rheumatoid arthritis and systemic lupus erythematosus. *N. Engl. J. Med.* 357:977–986. http://dx.doi.org/10.1056/NEJMoa073003

Santoro, A., S. Cannella, A. Trizzino, G. Bruno, C. De Fusco, L.D. Notarangelo, D. Pende, G.M. Griffiths, and M. Aricò. 2008. Mutations affecting mRNA splicing are the most common molecular defect in patients with familial hemophagocytic lymphohistiocytosis type 3. *Haematologica*. 93:1086–1090. http://dx.doi.org/10.3324/haematol.12622

Seo, J.Y., J.S. Song, K.O. Lee, H.H. Won, J.W. Kim, S.H. Kim, S.H. Lee, K.H. Yoo, K.W. Sung, H.H. Koo, et al; Korea Histiocytosis Working Party. 2013. Founder effects in two predominant intronic mutations of UNC13D, c.118-308C>T and c.754-1G>C underlie the unusual predominance of type 3 familial hemophagocytic lymphohistiocytosis (FHL3) in Korea. *Ann. Hematol.* 92:357–364. http://dx.doi.org/10.1007/s00277-012-1628-6

Serdobova, I., M. Pla, P. Reichenbach, P. Sperisen, J. Ghysdael, A. Wilson, J. Freeman, and M. Nabholz. 1997. Elf-1 contributes to the function of the complex interleukin (IL)-2-responsive enhancer in the mouse IL-2 receptor

alpha gene. *J. Exp. Med.* 185:1211–1221. http://dx.doi.org/10.1084/jem.185.7.1211

Shirakawa, R., T. Higashi, A. Tabuchi, A. Yoshioka, H. Nishioka, M. Fukuda, T. Kita, and H. Horiuchi. 2004. Munc13-4 is a GTP-Rab27-binding protein regulating dense core granule secretion in platelets. *J. Biol. Chem.* 279:10730–10737. http://dx.doi.org/10.1074/jbc.M309426200

Simon, J.M., P.G. Giresi, I.J. Davis, and J.D. Lieb. 2012. Using formaldehyde-assisted isolation of regulatory elements (FAIRE) to isolate active regulatory DNA. *Nat. Protoc.* 7:256–267. http://dx.doi.org/10.1038/nprot.2011.444

Thurman, R.E., E. Rynes, R. Humbert, J. Vierstra, M.T. Maurano, E. Haugen, N.C. Sheffield, A.B. Stergachis, H. Wang, B. Vernot, et al. 2012. The accessible chromatin landscape of the human genome. *Nature*. 489:75–82. http://dx.doi.org/10.1038/nature11232

Vahedi, G., H. Takahashi, S. Nakayamada, H.W. Sun, V. Sartorelli, Y. Kanno, and J.J. O'Shea. 2012. STATs shape the active enhancer landscape of T cell populations. *Cell*. 151:981–993. http://dx.doi.org/10.1016/j.cell.2012.09.044

Visconti, R., M. Gadina, M. Chiariello, E.H. Chen, L.F. Stancato, J.S. Gutkind, and J.J. O'Shea. 2000. Importance of the MKK6/p38 pathway for interleukin-12-induced STAT4 serine phosphorylation and transcriptional activity. *Blood*. 96:1844–1852.

Wei, L., G. Vahedi, H.W. Sun, W.T. Watford, H. Takatori, H.L. Ramos, H. Takahashi, J. Liang, G. Gutierrez-Cruz, C. Zang, et al. 2010. Discrete roles of STAT4 and STAT6 transcription factors in tuning epigenetic modifications and transcription during T helper cell differentiation. *Immunity*. 32:840–851. http://dx.doi.org/10.1016/j.immuni.2010.06.003

Wood, S.M., M. Meeths, S.C. Chiang, A.G. Bechensteen, J.J. Boelens, C. Heilmann, H. Horiuchi, S. Rosthøj, O. Rutynowska, J. Winiarski, et al. 2009. Different NK cell-activating receptors preferentially recruit Rab27a or Munc13-4 to perforin-containing granules for cytotoxicity. *Blood*. 114:4117–4127. http://dx.doi.org/10.1182/blood-2009-06-225359

Yamamoto, K., F. Shibata, N. Miyasaka, and O. Miura. 2002. The human perforin gene is a direct target of STAT4 activated by IL-12 in NK cells. *Biochem. Biophys. Res. Commun.* 297:1245–1252. http://dx.doi.org/10.1016/S0006-291X(02)02378-1

Yang, Y., J.C. Ochando, J.S. Bromberg, and Y. Ding. 2007. Identification of a distant T-bet enhancer responsive to IL-12/Stat4 and IFNgamma/Stat1 signals. *Blood*. 110:2494–2500. http://dx.doi.org/10.1182/blood-2006-11-058271

Yang, Y., D.M. Muzny, J.G. Reid, M.N. Bainbridge, A. Willis, P.A. Ward, A. Braxton, J. Beuten, F. Xia, Z. Niu, et al. 2013. Clinical whole-exome sequencing for the diagnosis of mendelian disorders. *N. Engl. J. Med.* 369:1502–1511. http://dx.doi.org/10.1056/NEJMoa1306555

Zhang, F., and M. Boothby. 2006. T helper type 1-specific Brg1 recruitment and remodeling of nucleosomes positioned at the IFN-gamma promoter are Stat4 dependent. *J. Exp. Med.* 203:1493–1505. http://dx.doi.org/10.1084/jem.20060066